

Heat Capacity Change of the Hydrophobic Interaction

Steven W. Rick[†]

Department of Chemistry, University of New Orleans, New Orleans, Louisiana 70148, and
Chemistry Department, Southern University of New Orleans, New Orleans, Louisiana 70126

Received: March 20, 2003; In Final Form: June 2, 2003

The thermodynamic properties of a methane pair in water are examined with use of molecular dynamics computer simulations. From the simulations, the heat capacity change for methane pair aggregation is examined for two different potential models. Various methods for calculating the heat capacity change are presented and evaluated. It is found that the heat capacity change for aggregation is negative, consistent with a positive heat capacity change for the aqueous solvation of nonpolar molecules.

Introduction

Two prominent features of the hydrophobic effect are the entropy change, ΔS , and the heat capacity change, ΔC_p .¹ This is demonstrated by the large and positive ΔS and ΔC_p for the solvation of nonpolar solutes in water.^{2,3} However, while the entropy change is significantly temperature dependent, the heat capacity change is not, and ΔS is positive for the solvation of polar solutes as well, while ΔC_p is negative, suggesting that the heat capacity change may be a more characteristic property of the hydrophobic effect.^{1,4} The heat capacity also shows a large increase for protein denaturing, possibly due to the increased contact between nonpolar groups and water.^{1,2,5} Determining heat capacity changes from computer simulations is a challenge and only a few studies have been reported, including studies on single particle hydration.^{4,6–8} A recent calculation reported that the heat capacity change is negative for the aggregation of small nonpolar molecules in water, consistent with the positive heat capacity change for the solvation of nonpolar molecules.⁹ A negative heat capacity change for aggregation of nonpolar solutes has also been reported experimentally.^{3,10,11} However, other computational studies, using different potential energy functions, found a positive ΔC_p .^{12–14} A positive ΔC_p for the hydrophobic interaction would suggest that the heat capacity is not such a characteristic property of hydrophobicity. These same studies found that the ΔC_p predicted from the solvent accessible surface area (SASA) or volume-based solvent exclusion models is negative.^{12,13} A study using a two-dimensional model found a negative heat capacity change.¹⁵ The sign of the heat capacity change then may depend on the potential model or the method used for its calculation. This is in contrast to the entropy change, for which many studies find to be positive.^{9,12–19}

The heat capacity is the second derivative of the free energy and so can be calculated by using three different numerical methods, depending on whether the derivatives are calculated analytically or numerically by finite difference,

$$\Delta C_p = -T \left\langle \left(\frac{\partial^2 \Delta G}{\partial T^2} \right)_{P,N} \right\rangle = \frac{1}{kT^2} (\langle \Delta H^2 \rangle - \langle \Delta H \rangle^2) \quad (1)$$

$$= \frac{\Delta H(T + \Delta T) - \Delta H(T - \Delta T)}{2\Delta T} \quad (2)$$

$$= \frac{-T(\Delta G(T + \Delta T) - 2\Delta G(T) + \Delta G(T - \Delta T))}{(\Delta T)^2} \quad (3)$$

Equation 1 is an analytic expression for the second derivative of ΔG , which relates ΔC_p to fluctuations in the enthalpy change, ΔH . Equation 2 evaluates one derivative analytically (to get ΔH) and the second through finite difference. Equation 3 expresses ΔC_p as a finite difference approximation to the second derivative, $-T(\partial^2 \Delta G / \partial T^2)_{P,N}$. These equations present three different methods for calculating ΔC_p . A fourth method is to fit the temperature dependence of ΔG to a functional form, such as

$$\Delta G(T) = \Delta H_0 + \Delta C_p(T - T_0) - T\Delta S_0 - T\Delta C_p \ln(T/T_0) \quad (4)$$

where ΔH_0 and ΔS_0 are entropy and enthalpy changes at a reference temperature, T_0 .^{1,2,12} Equations 3 and 4 both assume that ΔC_p is independent of temperature and give equivalent results if only three temperatures are used. Equation 2 makes the less restrictive approximation that the second temperature derivative of ΔC_p is zero and eq 1 makes no approximations regarding the temperature dependence. The previous calculations determined ΔC_p from the temperature dependence of ΔG .^{9,12,13} One comparison of ΔC_p at high pressures found that eqs 2 and 3 gave similar results.⁹

While the ΔC_p associated with the hydrophobic effect is often characterized as large (50 cal/(mol K⁻¹) and up),^{1,5} the magnitude is sufficiently small to make ΔC_p difficult to calculate. Over a temperature range of 30 K, the effect of nonzero ΔC_p on ΔG is only about 0.08 kcal/mol from eq 4 (using $T_0 = 283$ K, $T = 313$ K, and $\Delta C_p = 50$ cal/(mol K⁻¹)), which is comparable to the error bars on calculated ΔG values.^{12,19,20} Therefore, the deviation from linearity in the temperature dependence of ΔG is just barely outside the noise of the calculations. For this reason, earlier results lacked

[†] Address correspondence to the author at University of New Orleans.
E-mail: srick@uno.edu.

sufficient accuracy to provide quantitative estimates of ΔC_p .⁹ In this paper, we report calculations of ΔC_p using the eqs 1–3 for two different potential models. In addition, the free energies are computed with two different methods, through potential-of-mean-force (PMF) and thermodynamic integration (TI), in which the ΔG is found from a direct calculation of the free energy of the contact pair minus the free energy of an isolated solute, similar to previous test particle approaches.^{12,13,15,21,22}

Methods

The two potential models used are the all-atom polarizable fluctuating charge (FQ) model^{19,23} and the nonpolarizable model using the TIP4P water potential, the OPLS united-atom methane potential.^{24,25} Both models use the Lorentz–Berthelot combining rules for the Lennard-Jones parameters.²⁶ For both models, PMF calculations have been reported.^{9,12,13,19,27} Both these models give about the same solvation free energy^{12,19,28} (see also below), despite the fact that methane–water interactions are considerably different.¹⁹ In addition, the temperature dependence of many properties of the two water models are different^{29,30} so the two models are distinct enough to provide some estimate of the sensitivity of the results on the model. To evaluate eqs 2–4, free energy calculations were done at four temperatures: 283, 298, 313, and 328 K. The PMF calculations for the FQ model with umbrella sampling are as described previously,^{9,19} except (1) they use a larger system size (512 water and 2 methane molecules, so as to have a larger box size to follow the PMF out to larger separations), (2) they have a smaller separation (0.8 Å rather than 1.0 Å) between sampling windows to get better overlap, and (3) each of the 11 windows (evenly spaced from 4.0 to 12.0 Å) was simulated to 5.0 ns (7.5 ns at 283 K). The exact value of the PMF at the contact pair distance, $W(r_{CP})$, is sensitive to the value used for the zero free energy baseline¹² and also propagation of errors from the umbrella sampling result from the large separation to the contact pair. To get the most accurate value of $W(r_{CP})$ we use thermodynamic integration (TI). The ΔG from TI was found in two parts, as described below. The PMF force was calculated from the biased umbrella sampling data with use of the weighted histogram method,^{31,32} with the added restraints that the PMF is equal to the TI value at $W(r_{CP})$ and equal to zero at $r = 12$ Å. The TI calculations evaluated the standard free energy integral

$$\Delta G = \int_0^1 \left\langle \frac{\partial E_\lambda}{\partial \lambda} \right\rangle_\lambda d\lambda \quad (5)$$

with about 10 ns of data collection for each 12 integration points along λ and used separated-shifted scaling to eliminate possible singularities as λ approaches zero.^{33,34} The entropy change was calculated from the temperature derivative of eq 5,^{6,16,35}

$$\Delta S = \frac{-1}{kT^2} \int_0^1 \left(\left\langle (PV + E_\lambda) \frac{\partial E_\lambda}{\partial \lambda} \right\rangle_\lambda - \langle PV + E_\lambda \rangle_\lambda \left\langle \frac{\partial E_\lambda}{\partial \lambda} \right\rangle_\lambda \right) d\lambda \quad (6)$$

and the heat capacity change from eq 1 is given by

$$\begin{aligned} \Delta C_p = & -2\Delta S - \frac{1}{k^2 T^3} \int_0^1 \left(\left\langle (PV + E_\lambda)^2 \frac{\partial E_\lambda}{\partial \lambda} \right\rangle_\lambda - \right. \\ & 2\langle PV + E_\lambda \rangle_\lambda \left\langle (PV + E_\lambda) \frac{\partial E_\lambda}{\partial \lambda} \right\rangle_\lambda - \langle (PV + E_\lambda)^2 \rangle_\lambda \left\langle \frac{\partial E_\lambda}{\partial \lambda} \right\rangle_\lambda + \\ & \left. 2\langle PV + E_\lambda \rangle_\lambda^2 \left\langle \frac{\partial E_\lambda}{\partial \lambda} \right\rangle_\lambda \right) d\lambda \quad (7) \end{aligned}$$

TABLE 1: Free Energy Changes from Thermodynamic Integration (kcal/mol) for Four Different Temperatures and Showing the Results for Two Different Models, the Polarizable Fluctuating Charge Model and the Nonpolarizable TIP4P-OPLS Model

<i>T</i> (K)	FQ polarizable model			TIP4P-OPLS model		
	ΔG_1	ΔG_2	$W(r_{CP})$	ΔG_1	ΔG_2	$W(r_{CP})$
283	2.11(3)	1.64(3)	−0.47(4)	2.08(2)	1.52(2)	−0.55(3)
298	2.38(3)	1.74(2)	−0.64(3)	2.28(2)	1.63(2)	−0.65(3)
313	2.56(2)	1.85(2)	−0.71(3)	2.44(2)	1.69(2)	−0.76(3)
328	2.68(2)	1.83(2)	−0.86(3)	2.51(2)	1.72(2)	−0.79(2)

The simulations were done in the isothermal–isobaric (constant T , P , N) ensemble, by coupling to a pressure bath and a Nosé–Hoover temperature bath at temperatures of 283, 298, and 313 K.^{36–40} All simulations used a 1 fs times step, the Ewald sum for long-ranged electrostatic interactions, and SHAKE for bond constraints.²⁶ The TI calculations contained 256 solvent molecules. All error bars represent 95% confidence limits.

Results

The TI results for ΔG are given in Table 1. The value of the PMF at r_{CP} , $W(r_{CP})$, can be found from

$$W(r_{CP}) = \Delta G_2 - \Delta G_1 \quad (8)$$

where ΔG_1 is the free energy of adding a single methane to the pure solvent and ΔG_2 is the free energy of adding a second a distance r_{MM} ($r_{MM} = 3.8$ Å) away from the first methane. The single particle free energy changes for both potential models are in good agreement with previous calculations and with the experimental value (2.0 kcal/mol).^{12,19,28,41} The potential of mean force, $W(r)$, at three different temperatures is shown in Figure 1A. Also plotted are the thermodynamic integration results, which the $W(r)$ values are constrained to pass through. The potential of mean force has a minimum, the contact pair minimum, at 3.8 Å, as well as another local minimum, the solvent separated pair minimum, at 7 Å, and a well-defined barrier between the two around 5.5 Å, as has been demonstrated previously in a number of different studies.^{9,12,17–20,27,42–52} The potential of mean force also has structure at least out to 11 Å showing another barrier around 9 Å and another minimum around 10 Å. The long-ranged structure of $W(r)$ has been shown previously in a small number of studies.^{9,12,18,27} The free energy of the contact pair decreases as the temperature is increased, which is indicative of a process with a positive entropy change. The free energy of the solvent separated pair does not show a large temperature dependence. This temperature dependence is in agreement with previous studies.^{12,17–20} One subtle feature of $W(r)$ is a slight outward shift of the position of the barrier maximum and the solvent separated pair minimum with increasing temperature. This shift appears to be largest at the barrier position. The barrier region represents a structure in which the methane pairs are not in contact but there is not enough room to put a solvent molecule.^{17,53} Therefore, the barrier region contains relatively more open space than other configurations and is likely to be more compressible. A small outward shift in the position of the barrier with increasing temperature, at constant pressure, is also present in the results of Shimizu and Chan,¹² but not present in the constant volume results of Lüdemann et al.¹⁸ The shift is consistent with the decrease in density (an increase in molecular volume) with temperature (above 4 K), which is present both in real water and in the models used here.^{29,30}

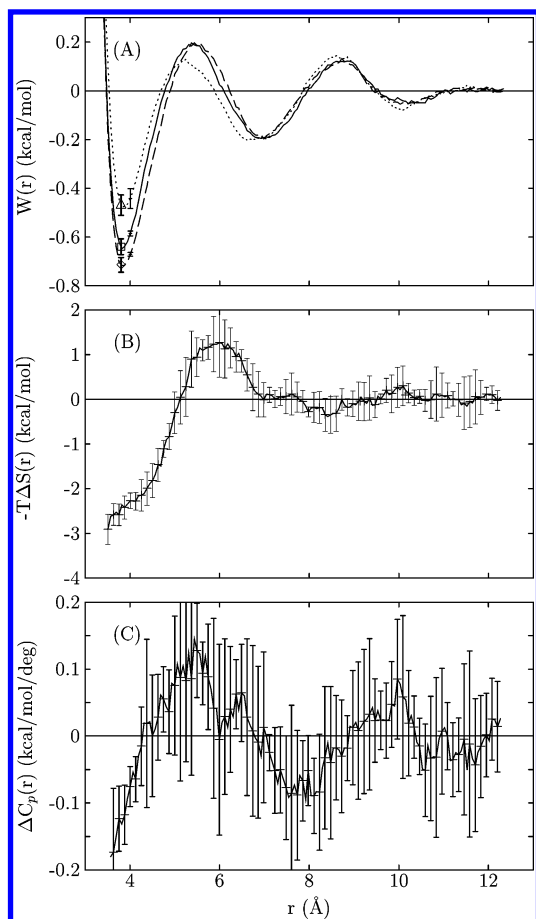


Figure 1. (A) Methane pair potential of mean force for the polarizable FQ model at 283 (dotted line), 298 (solid line), and 313 K (dashed line) as a function of methane separation, r , and values from thermodynamic integration for $r = 3.8$ Å at 283 (diamond), 298 (square), and 313 K (triangle). Error bars are shown at 4.0 Å. (B) Entropic contribution to $W(r)$ at 298 K. (C) Heat capacity change, $\Delta C_p(r)$, at 298 K.

TABLE 2: Entropy Changes from Thermodynamic Integration (kcal/mol) for Three Different Temperatures and Showing the Results for Two Different Models

T (K)	FQ polarizable model			TIP4P-OPLS model		
	$-T\Delta S_1$	$-T\Delta S_2$	$-T\Delta S(r_{CP})$	$-T\Delta S_1$	$-T\Delta S_2$	$-T\Delta S(r_{CP})$
283	6.5(1.1)	1.1(1.1)	-5.4(1.5)	3.5(5)	1.6(5)	-1.9(7)
298	4.5(9)	0.6(9)	-3.9(1.2)	2.6(4)	1.2(5)	-1.4(6)
313	2.3(8)	-0.3(7)	-2.7(1.1)	1.5(5)	0.4(4)	-1.2(6)

The entropy changes from eq 6 are given in Table 2. The entropy for solvating a single methane molecule, ΔS_1 , for both models, at 298 K, is comparable to other calculated values^{6,54} and to the experimental value, $-T\Delta S = 4.8$ kcal/mol.⁴¹ From the PMF results, the entropy change as a function of methane pair distance can be found from finite difference,²⁰

$$-T\Delta S(r) = \frac{T[W(r, T+\Delta T) - W(r, T-\Delta T)]}{2\Delta T} \quad (9)$$

The entropy (Figure 1B) shows the entropic stabilization of the contact pair and an entropic barrier around 6 Å, in agreement with previous studies.^{9,13,15–20} An experimental estimate, based on the difference of the standard entropy of solution of ethane and two methane molecules, gives $-T\Delta S(r_{CP}) = -3.6$ kcal/mol.³ This value is similar to the entropy changes found here and elsewhere.^{12,19,20} The entropy change can also be calculated directly from the PMF through an equation similar to eq 6,²⁰

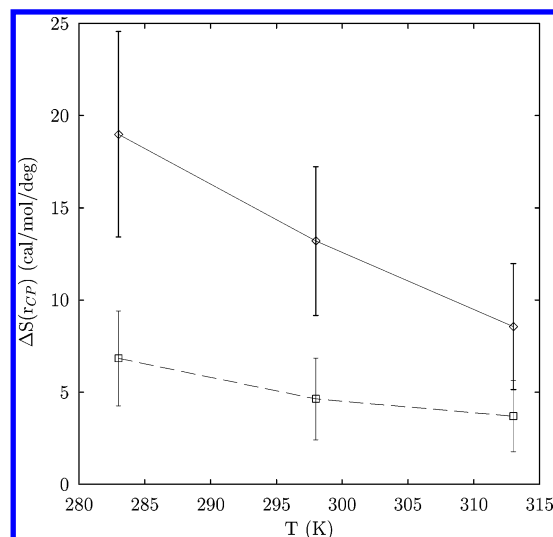


Figure 2. Entropy change for forming the contact pair, calculated from thermodynamic integration (eq 6), as a function of temperature for the polarizable FQ model (solid lines and diamonds) and the TIP4P-OPLS model (dashed line and squares).

but for the size system used here the noise was too large to provide meaningful estimates of the entropy.

All the entropic contributions to the free energies ($-T\Delta S_1$, $-T\Delta S_2$, and $-T\Delta S(r_{CP})$) increase with temperature, or ΔS decreases with temperature (Figure 2). The decrease in ΔS_1 is consistent with the entropy changes for the solvation of nonpolar solutes, all which decrease with temperature and reach zero at a temperature, T_S , equal to 410 ± 40 K.^{2,5} If $-T\Delta S(r_{CP})$ is linearly extrapolated, the entropy change should become zero at 343 K for the FQ model and 357 K for the TIP4P-OPLS model, reasonably close the experimental T_S considering the linear extrapolation probably underestimates T_S .² A recent information theory model of solvation indicates that the temperature dependence of free energies for hydrophobic hydration is determined largely by the temperature dependence of the liquid density, ρ .^{55,56} The theory predicts that T_S should be proportional to $1/\alpha$, where α is the coefficient of thermal expansion, $\alpha = -(1/\rho)(\partial\rho/\partial T)_{P,N}$. This result provides a possible explanation for the fact that both the potential models used here underestimate T_S . From the published temperature dependences of ρ ,^{29,30} values of α can be found and both models have values which are too high ($56 \pm 6 \times 10^{-5}$ K⁻¹ for TIP4P⁵⁷ and $60 \pm 7 \times 10^{-5}$ K⁻¹ for TIP4P-FQ,⁵⁸ compared to the experimental value of 25.7×10^{-5} K⁻¹⁵⁹). The decrease in $\Delta S(r_{CP})$ over a broad range of temperature (up to 500 K) has also been reported by Lüdemann et al.¹⁸ Those results give a T_S between 400 and 500 K, although this is at elevated pressures, and the pressure may effect the entropy changes.⁹ The decrease in $\Delta S(r_{CP})$ means a negative heat capacity, since $\Delta C_p = T(\partial\Delta S/\partial T)_{P,N}$.

The heat capacity changes are given in Table 3. There is a fair degree of statistical uncertainty in the results, but there is general agreement between the various methods and potential models that ΔC_p at the contact pair position is negative. These are the largest errors using the direct method (eqs 1 and 7). At $T = 298$ K, for the FQ model, from eqs 1 and 7, $\Delta C_{P,1} = -0.01 \pm 0.17$ kcal/(mol deg⁻¹) and $\Delta C_{P,2} = 0.05 \pm 0.19$ kcal/(mol deg⁻¹) and for the TIP4P-OPLS model, $\Delta C_{P,1} = -0.05 \pm 0.11$ kcal/(mol deg⁻¹) and $\Delta C_{P,2} = 0.01 \pm 0.09$ kcal/(mol deg⁻¹). The value for ΔC_p is found from $\Delta C_{P,2} - \Delta C_{P,1}$. Equation 4 gives the smallest error bars, but makes the largest physical approximation, that ΔC_p is independent of temperature over a range from 283 to 328 K. Equation 3 gives error bars

TABLE 3: Heat Capacity Change for the Formation of the Contact Pair as Calculated from Thermodynamic Integration with the Four Different Methods and the Weighted Average for the Two Different Potential Models (kcal/(mol deg⁻¹))

	eq 1	eq 2	eq 3	eq 4	av
FQ model	0.05(0.26)	-0.098(0.070)	-0.13(0.11)	-0.012(0.046)	-0.045(0.042)
TIP4P-OPLS	0.06(0.14)	-0.033(0.044)	0.011(0.082)	-0.048(0.034)	-0.034(0.029)

slightly larger than eq 4 and does not assume that ΔC_P is independent of temperature. All four estimates can be averaged together, using $\Delta C_{P,\text{ave}} = (\sum_i \Delta C_{P,i} / \sigma_i^2) / (\sum_i 1 / \sigma_i^2)$, where the sum is over the four estimates of ΔC_P and σ is the error estimate for that method. This gives -0.045 ± 0.042 kcal/(mol deg⁻¹) for the FQ model and -0.034 ± 0.029 kcal/(mol deg⁻¹) for the TIP4P-OPLS model.⁶⁰ The experimental estimate from the difference in the ΔC_P of hydration between ethane and two methane molecules is -0.038 kcal/(mol deg⁻¹).³ An estimate of ΔC_P can also be found from fitting the data shown in Figure 2 to a straight line and using the slope. This gives values that are identical with the values from eq 2 with slightly smaller error bars, since it uses one more data point ($\Delta C_P = -0.10 \pm 0.06$ kcal/(mol deg⁻¹) for FQ and -0.03 ± 0.03 kcal/(mol deg⁻¹) for TIP4P-OPLS).

The heat capacity as a function of distance, $\Delta C_P(r)$, and $W(r)$ can be used to find the heat capacity for the methane pair in the region of the contact pair free energy minimum. The average heat capacity change for the contact pair region can be found from the Boltzmann weighted average of $\Delta C_P(r)$ over this region,

$$\langle \Delta C_P \rangle_{\text{CP}} = \frac{\int_{r_A}^{r_B} e^{-W(r)/kT} \Delta C_P(r) 4\pi r^2 dr}{\int_{r_A}^{r_B} e^{-W(r)/kT} 4\pi r^2 dr} \quad (10)$$

where r_A is 3.3 Å and r_B is 5.4 Å [this is the position of the maximum of $W(r)$]. This gives a value of $\langle \Delta C_P \rangle_{\text{CP}}$ equal to -0.029 ± 0.014 kcal/(mol deg⁻¹). (This is for the FQ model.)

The $\Delta C_P(r)$ from the PMF shows a fair amount of structure, as has been seen previously (Figure 1C).^{13–15} The most significant feature of $\Delta C_P(r)$ is the decrease from a positive value at the barrier region of $W(r)$, around 5.5 Å, to a negative value at the contact pair free energy minimum. A large shift in $\Delta C_P(r)$ in this region is seen in other studies.^{13–15} This is the region where $W(r)$ and $\Delta S(r)$ both change the most. It is worth emphasizing that the region around 5.5 Å, where $\Delta C_P(r)$ is positive, corresponds to a free energy maximum, representing a thermodynamically unstable geometry with an increased amount of free volume. The width and height of the barrier changes significantly with pressure^{9,61,62} and the barrier region is also apparently sensitive to temperature, as indicated by the peaks in $-T\Delta S(r)$ and $\Delta C_P(r)$. Another minimum in $\Delta C_P(r)$ occurs at larger separations, which is not quite coincident with the solvent separated pair minimum of $W(r)$ (at 7 Å) but at a slightly larger separation (around 8 Å). A similar outward shift in this minimum of $\Delta C_P(r)$ relative to the minimum of $W(r)$ may also be present in the results of Shimizu and Chan^{13,14} and Southall and Dill,¹⁵ although in all cases the error bars are too large to identify the position of this minimum with much accuracy. Overall, the $\Delta C_P(r)$ in Figure 1C looks qualitatively similar to the results of Shimizu and Chan, with the notable exception that the value at the contact pair is negative relative to the pair at large (12 Å) separations, which Shimizu and Chan report to be positive. The present result for $\Delta C_P(r)$ is the least uncertain at $r = r_{\text{CP}}$, since this point was adjusted against the thermodynamic integration results. The differences between the present results and those of Shimizu and Chan, which use the

same TIP4P-OPLS model as presented here, are most likely due to the fact that they find ΔC_P from $W(r)$ over a broad range of temperature, from 278 to 388 K, assuming a constant ΔC_P over this range, while the present results use a much smaller temperature range. The heat capacity change for the solvation of nonpolar molecules is temperature dependent, decreasing with increasing temperature,² so the Shimizu and Chan estimate of ΔC_P at 298 K may be changed by the high-temperature data. The present results are also significantly different from earlier results which lacked sufficient accuracy to give good estimates of the heat capacity, demonstrating the difficulty of finding $\Delta C_P(r)$ from the $W(r)$ at different temperatures.⁹

Conclusion

Using four different computational approaches and two different potential models, our results suggest that the heat capacity change for bringing two methane molecules together is *negative*. The heat capacity as a function of solute separation demonstrates a global minimum at the contact pair separation and another minimum near the solvent separated separation. The $-T\Delta S(r)$ and $\Delta C_P(r)$ functions show an agreement between the regions with the most disorder (smallest $-T\Delta S$) and lowest ΔC_P (the contact pair) and with the most order and highest ΔC_P (the barrier region around 5.5 Å, see Figure 1, parts B and C). Thus there seems to be a correlation between the amount of disorder and the number of thermally accessible microstates. (See refs 1, 4, 8, 5, 2, 3, and 63 for more on the connections between entropy and heat capacity for hydrophobic interactions.) The negative ΔC_P is consistent with the positive heat capacity change for the solvation of nonpolar molecules.^{2,3} A well-known feature of hydrophobicity is entropy convergence, in which the entropy of solvation for nonpolar molecules, positive at 25 K, decreases and reaches zero at about the same temperature.^{2,5} This implies that entropy changes for hydrophobic processes, including aggregation, are zero at this temperature. If the entropy change for the hydrophobic association is positive at 25 K, as a consensus of studies find, then, if ΔS is a monotonic function of temperature over this range, $(\partial \Delta S / \partial T)$ and, therefore, C_P must be negative. The negative ΔC_P is consistent as well with the interpretation of the increase in C_P upon protein denaturation as being due to the exposure of nonpolar residues to water.^{1,2}

Acknowledgment. Support from the Louisiana Board of Regents under contract number LEQSF(2001-04)-RD-A-42 and the National Science Foundation under contract number CHE-0213488 is gratefully acknowledged.

References and Notes

- (1) Dill, K. A. *Biochemistry* **1990**, 29, 7133.
- (2) Privalov, P. L.; Gill, S. J. *Adv. Protein Chem.* **1988**, 39, 191–234.
- (3) Ben-Naim, A. *Hydrophobic Interactions*; Plenum: New York 1980.
- (4) Sharp, K. A.; Madan, B. *J. Phys. Chem. B* **1997**, 101, 4343–4348.
- (5) Baldwin, R. L. *Proc. Natl. Acad. Sci. U.S.A.* **1986**, 83, 8069–8072.
- (6) Guillot, B.; Guissani, Y. *J. Chem. Phys.* **1993**, 99, 8075–8094.
- (7) Vanzi, F.; Madan, B.; Sharp, K. J. *Am. Chem. Soc.* **1998**, 120, 10748–10753.
- (8) Arthur, J. W.; Haymet, A. D. J. *J. Chem. Phys.* **1999**, 110, 5873–5883.
- (9) Rick, S. W. *J. Phys. Chem. B* **2000**, 104, 6884–6888.

- (10) Christian, S. D.; Tucker, E. E. *J. Solution Chem.* **1982**, *11*, 749–754.
- (11) Matulis, D. *Biophys. Chem.* **2001**, *93*, 67–82.
- (12) Shimizu, S.; Chan, H. S. *J. Chem. Phys.* **2000**, *113*, 4683–4700; **2002**, *116*, 8636.
- (13) Shimizu, S.; Chan, H. S. *J. Am. Chem. Soc.* **2001**, *123*, 2083–2084.
- (14) Shimizu, S.; Chan, H. S. *Proteins* **2002**, *49*, 560–566.
- (15) Southall, N. T.; Dill, K. A. *Biophys. Chem.* **2002**, *101–102*, 295–307.
- (16) Smith, D. E.; Zhang, L.; Haymet, A. D. J. *J. Am. Chem. Soc.* **1992**, *114*, 5875.
- (17) Jungwirth, P.; Zahradnik, R. *Chem. Phys. Lett.* **1994**, *217*, 319–324.
- (18) Lüdemann, S.; Abseher, R.; Schreiber, H.; Steinhauser, O. *J. Am. Chem. Soc.* **1997**, *119*, 4206–4213.
- (19) Rick, S. W.; Berne, B. J. *J. Phys. Chem. B* **1997**, *101*, 10488.
- (20) Smith, D. E.; Haymet, A. D. J. *J. Chem. Phys.* **1993**, *98*, 6445.
- (21) Ben-Naim, A. *Solvation Thermodynamics*; Plenum: New York 1987.
- (22) Forsman, J.; Jönsson, B. *J. Chem. Phys.* **1994**, *101*, 5116–5125.
- (23) Rick, S. W.; Stuart, S. J.; Berne, B. J. *J. Chem. Phys.* **1994**, *101*, 6141.
- (24) Jorgensen, W.; Chandrasekhar, J.; Madura, J. D.; Impey, R. W.; Klein, M. L. *J. Chem. Phys.* **1983**, *79*, 926.
- (25) Jorgensen, W. L.; Madura, J. D.; Swenson, C. J. *J. Am. Chem. Soc.* **1984**, *106*, 6638.
- (26) Allen, M. P.; Tildesley, D. J. *Computer Simulation of Liquids*; Oxford University Press: Oxford, UK, 1987.
- (27) Lüdemann, S.; Schreiber, H.; Abseher, R.; Steinhauser, O. *J. Chem. Phys.* **1996**, *104*, 286–295.
- (28) Jorgensen, W. L.; Blake, J. F.; Buckner, J. K. *Chem. Phys.* **1989**, *129*, 193.
- (29) Jorgensen, W. L.; Jensen, C. *J. Comput. Chem.* **1998**, *19*, 1179–1186.
- (30) Rick, S. W. *J. Phys. Chem.* **2001**, *114*, 2276–2283.
- (31) Ferrenberg, A. M.; Swendsen, R. H. *Phys. Rev. Lett.* **1989**, *63*, 1195.
- (32) Kumar, S.; Bouzida, D.; Swendsen, R. H.; Kollman, P. A.; Rosenberg, J. M. *J. Comput. Chem.* **1992**, *13*, 1011.
- (33) Zacharias, M.; Straatsma, T. P.; McCammon, J. A. *J. Chem. Phys.* **1994**, *100*, 9025–9031.
- (34) Rick, S. W.; Berne, B. J. *J. Am. Chem. Soc.* **1996**, *118*, 672.
- (35) Yu, H.; Karplus, M. *J. Chem. Phys.* **1988**, *89*, 2366–2379.
- (36) Andersen, H. C. *J. Chem. Phys.* **1980**, *72*, 2384.
- (37) Ciccotti, G.; Ryckaert, J. P. *Comput. Phys. Rep.* **1986**, *4*, 345.
- (38) Martyna, G. J.; Tobias, D. J.; Klein, M. L. *J. Chem. Phys.* **1994**, *101*, 4177.
- (39) Nosé, S. *Mol. Phys.* **1984**, *52*, 255.
- (40) Hoover, W. G. *Phys. Rev. A* **1985**, *31*, 1695.
- (41) Ben-Naim, A.; Marcus, Y. *J. Chem. Phys.* **1984**, *81*, 2016–2027.
- (42) Pratt, L. R.; Chandler, D. *J. Chem. Phys.* **1977**, *67*, 3683.
- (43) Pangali, C.; Rao, M.; Berne, B. J. *J. Chem. Phys.* **1979**, *71*, 2975.
- (44) Swaminathan, S.; Beveridge, D. L. *J. Am. Chem. Soc.* **1979**, *101*, 5832.
- (45) Rapaport, D. C.; Scheraga, H. A. *J. Phys. Chem.* **1982**, *86*, 873.
- (46) Watanabe, K.; Andersen, H. C. *J. Phys. Chem.* **1986**, *90*, 795.
- (47) Jorgensen, W. L.; Buckner, J. K.; Boudon, S.; Tirado-Rives, J. *J. Chem. Phys.* **1988**, *89*, 3742.
- (48) van Belle, D.; Wodak, S. J. *J. Am. Chem. Soc.* **1993**, *115*, 647.
- (49) Dang, L. X. *J. Chem. Phys.* **1994**, *100*, 9032.
- (50) Head-Gordon, T. *Chem. Phys. Lett.* **1994**, *227*, 215.
- (51) New, M. H.; Berne, B. J. *J. Am. Chem. Soc.* **1995**, *117*, 7172.
- (52) Young, W. S.; Brooks, C. L., III. *J. Chem. Phys.* **1997**, *106*, 9265.
- (53) Zichi, D. A.; Rossky, P. J. *J. Chem. Phys.* **1985**, *83*, 797–808.
- (54) Guillot, B.; Guissani, Y.; Bratos, S. *J. Chem. Phys.* **1991**, *95*, 3643–3648.
- (55) Garde, S.; Hummer, G.; García, A. E.; Paulaitis, M. E.; Pratt, L. R. *Phys. Rev. Lett.* **1996**, *77*, 4966–4968.
- (56) Pratt, L. R. *Annu. Rev. Phys. Chem.* **2002**, *53*, 409–436.
- (57) The compressibility was calculated from the density data from ref 29, using the values at 12.5, 25.0, and 37.5 °C and error bars for density equal to 0.001 g/cm³.
- (58) The compressibility was calculated from the density data from ref 30, using the values at 290, 298, and 310 K and error bars for density equal to 0.001 g/cm³.
- (59) Kell, G. S. *J. Chem. Eng. Data* **1975**, *20*, 97–105.
- (60) The error estimate was made assuming the estimates from eqs 1, 2, and 3 are statistically uncorrelated and the estimates from eqs 3 and 4 have a correlation coefficient equal to ³/₄, since they share ³/₄ of the same ΔG data.
- (61) Payne, V. A.; Matubayashi, N.; Murphy, L. R.; Levy, R. M. *J. Phys. Chem. B* **1997**, *101*, 2054–2060.
- (62) Hummer, G.; Garde, S.; García, A. E.; Paulaitis, M. E.; Pratt, L. R. *Proc. Natl. Acad. Sci.* **1998**, *95*, 1552–1555.
- (63) Southall, N. T.; Dill, K. A.; Haymet, A. D. J. *J. Phys. Chem. B* **2002**, *106*, 521–533.